Journal of Applied Polymer Science

A regioregular polythiophene–fullerene for polymeric solar cells

Massimiliano Lanzi, Elisabetta Salatelli, Tiziana Benelli, Daniele Caretti, Loris Giorgini, Francesco Paolo Di-Nicola

Dipartimento di Chimica Industriale "Toso Montanari", Università di Bologna, Viale del Risorgimento, 4 I-40136 Bologna, Italy

This work is dedicated to the memory of Prof. Paolo Costa Bizzarri.

Correspondence to: M. Lanzi (E-mail: massimiliano.lanzi@unibo.it)

ABSTRACT: In this article, we present the synthesis and characterization of a new thiophenic copolymer bearing the C_{60} fullerene directly linked to the end of a hexamethylenic side chain. This copolymer was prepared with good yield using a simple and straightforward post-polymerization functionalization procedure applied on a soluble regioregular polymeric precursor obtained by regiospecific organometallic coupling. Copolymer structural and photophysical properties were investigated by gel permeation chromatography, thermal analysis (DSC and TGA), NMR, IR, UV–Vis, and atomic force spectroscopy. The double-cable copolymer possesses good solubility in common organic solvents, high filmability, thermal stability, and low segmental aggregation tendency. It was tested as a photoactive layer in a polymeric solar cell showing a power conversion efficiency under 100 mW cm^{-2} AM 1.5 illumination higher than 4%, more than that of the reference cell made with the conventionally used P3HT/PCBM blend. © 2015 Wiley Periodicals, Inc. J. Appl. Polym. Sci. **2015**, *132*, 42121.

KEYWORDS: conducting polymers; functionalization of polymers; graphene and fullerenes; nanotubes; optical and photovoltaic applications

Received 3 November 2014; accepted 15 February 2015

DOI: 10.1002/app.42121

INTRODUCTION

Organic photovoltaic (OPV) solar cells are devices based on either small organic semiconducting molecules or conjugated polymers capable of converting sunlight into electrical power. They are prepared by sandwiching a thin (from tens to a few hundred nanometers) film of an organic semiconductor between two electrodes. In the usual geometry, the electrons exit from the top electrode (usually Al) and positive holes from the bottom electrode (usually ITO which, thanks to its high transparency, allows for a good illumination of the photo-active layer); however, an inverted geometry has also been reported, in which electrons exit at the bottom and holes at the top.[1–3] The active layer, made by intermixing an electron–acceptor and an electron–donor material, is usually deposited either by spin-coating a solution of conjugated polymer/electron acceptor molecule on the ITO electrode or by vacuum-evaporating small organic molecules on the same substrate. In the latter case, some active materials can be easily synthesized and purified, thus increasing the photoconversion efficiency, while the processing speed is usually lower than for solution-processed conjugated polymers.[4] In any case, OPV solar cells are very attractive devices, being cost-effective, light-weight, and particularly suitable for being scaled-up from a laboratory scale (usually a few square centimeters) to a commercial scale (many square meters) using roll-to-roll printing techniques.[5]

Among the different possible techniques for fabricating OPV cells, bulk heterojunction (BHJ) architecture has been studied intensively in recent years for its potential to obtain high efficiency at low costs. BHJ is essentially based on a bi-continuous network of an electron-donor (a conjugated polymer) and acceptor (fullerene or its derivatives) in which the two components are separated at a micro- or nanoscale level, with a high internal surface area where the ultrafast photoinduced charge transfer can occur; this way mobile holes in the donor phase and mobile electrons in the acceptor phase can be generated. The carriers produced are then driven to the electrodes by the cell internal field before they recombine in the photoactive layer.

The carrier generation and transport process is the key-mechanism which determines the main parameters of the BHJ

Additional Supporting Information may be found in the online version of this article.

solar cell, directly acting on the short-circuit current density (J_{sc}), the fill factor (FF), and then the final power conversion efficiency (PCE).

The morphology and microstructure of the active layer are thus of primary importance, even if how to control them and at what degree of separation remain unclear, as a compromise is required between the need for a nanoscale separation (i.e., high interfacial area) for efficient exciton quenching, and the presence of larger domains (macrophase separation) for both the efficient transport of charges to the electrodes and an increased carrier lifetime.[6]

With the aim of producing optimal phase segregation between the donor and acceptor molecules for charge generation while, at the same time, maintaining a continuous path in each phase for the efficient transport of electrons and holes, a number of strategies have been adopted. Among them, the synthesis of donor–acceptor double-cable polymers appears particularly intriguing. In fact, this architecture leads to the homogeneous distribution of the electron donor-acceptor (ED-EA) domains, at the same time maximizing the interface between them.[7] In these systems, the fullerene group is usually linked to the conjugated polymer (CP) main chain (generally a polythiophene derivative, exploiting the 3-position of the thiophenic units) by means of either an aromatic substituent[8] or an alkylic spacer which enhances the solubility of the final polymer by increasing the mobility of the EA group and, at the same time, electronically insulates the conjugated backbone from the C_{60} aromatic molecule.[9,10]

Double-cable polymers allow for the optimized nanoscale phase separation of the EA/ED domains whose length scale must be comparable to exciton diffusion distance (10–20 nm[11]) by avoiding spontaneous phase separation; the latter is usually observed in conventional BHJ blends, and is caused by the very low entropy of mixing for high molecular weight polymers.[12]

On these bases, the making of a "molecular heterojunction" by covalently grafting fullerene to polythiophene backbone may be considered a suitable alternative to the conventional BHJ architecture of OPV solar cells; in fact, this system exploits the same ED/EA moieties while retaining the positive electronic and photophysical properties of CP/fullerene composites but limiting phase separation and clustering phenomena. A drawback of double-cable polymer way to build polymeric solar cells is, indeed, the more complex synthetic route necessary to obtain the fullerene-functionalized monomers; this usually makes the conventional BHJ architecture—based on the simple mixing of the ED/EA components even if on a nanoscale separation—preferable when final power conversion efficiencies are essentially the same.

In this article, we report on both the synthesis of a new thiophenic monomer bearing the C_{60}-fullerene at the end of a hexylic side chain, and the preparation of a soluble thiophenic copolymer using the same procedure used for the monomer on a reactive polymeric precursor. The synthesis used is particularly interesting as it involves a very simple and straightforward procedure based on the Grignard-coupling between ω-bromoalkyl-derivatives and C_{60}-fullerene. The prepared copolymer was widely characterized using IR, NMR, GPC, UV–Vis spectroscopy, and DSC-TGA thermal analysis. The molecular arrangement of its thin films was studied by AFM measurements. Lastly, the current density/voltage (J/V) characteristics of the prepared solar cell were determined under one-sun illumination, to evaluate PCE when using the newly synthesized double-cable copolymer as a photoactive layer; these characteristics were also compared with those of a reference OPV solar cell made with BHJ conventional architecture.

EXPERIMENTAL

Materials

All reagents were purchased from Sigma–Aldrich Chemical and used without further purification where not expressly indicated otherwise. All solvents used (HPLC grade) were dried and purified by normal procedures, stored under molecular sieves, and handled in a moisture-free atmosphere.

The reference polymer for solar cells, that is, poly(3-hexylthiophene) (P3HT), was synthesized starting from 3-hexylthiophene (T6H) purchased from Sigma–Aldrich (CAS No. 1693-86-3, Product No. 399051) using the McCullough procedure,[13] regioregularity in HT dyads 96%, M_n 30.0 kDa, PDI 1.2.

Measurements

^{1}H-NMR and ^{13}C-NMR were recorded on a Varian Mercury Plus spectrometer using TMS as a reference. IR spectra were taken on KBr pellets (model compound and alkylthiophene–fullerene derivative) and Ge disk (thin polymer films) using a Perkin Elmer Spectrum One spectrophotometer. Molecular weights were determined by gel permeation chromatography (GPC) using polystyrene standards and THF as an eluent on a HPLC Lab Flow 2000 apparatus equipped with a PL Gel MXL column and a Linear Instrument UV–Vis detector model UVIS-200 working at 263 nm. Mass spectra were recorded on a Thermo Finnigan MAT95XP spectrometer. The elemental analysis of the prepared copolymers was performed by Redox Laboratory, Monza, Italy. UV–Vis spectra were recorded on a Perkin Elmer Lambda 19 spectrophotometer using polymer films on quartz slides cast from o-dichlorobenzene (ODCB) solutions using the doctor blading (DB) technique (average thickness: 150 nm). A DSC TA Instruments 2920 was used for the thermal analysis of the polymer by varying the temperature from −50 to 200°C at a rate of 10°C min^{-1} in a nitrogen atmosphere. A TGA TA Instruments 2050, operating in either an inert or an oxidizing atmosphere, was used to determine the decomposition temperatures of the polymer by heating samples from 30 to 900°C at a heating scan rate of 20°C min^{-1}. AFM measurements were made on a Burleigh Vista instrument in a non-contact tapping mode using high resolution silicon-nitride tips.

For the preparation of the solar cells, ITO glass (1 × 1 cm^2) was first cleaned in an ultrasonic bath using a non-foaming glass detergent in deionized water. ITO glass was then rinsed sequentially in double distilled water, isopropanol, and acetone. PEDOT:PSS (Aldrich Chemical) was diluted 1 : 1 with isopropanol, filtered on a Gooch filter G2, and deposited by doctor blading on top of the cleaned ITO glass (film thickness about

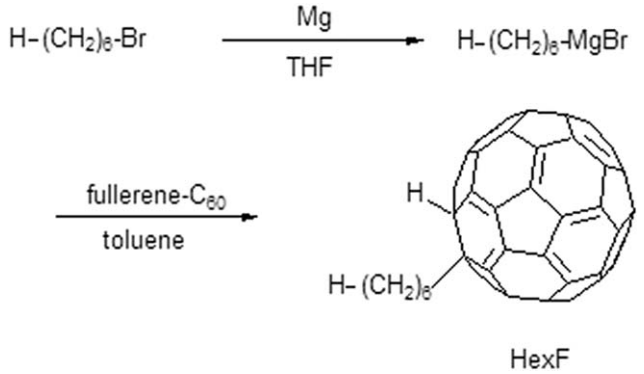

Scheme 1. Synthesis route for the preparation of HexF.

80 nm) by means of a Sheen Instruments S265674. The glass slide was baked under a vacuum at 120°C for 2 h using a Büchi GKR-50 Micro Glass Oven. Anhydrous ODCB was used to prepare solutions of COP2 (7, 10, 13, and 15 mg ml^{-1}), which were deposited by doctor blading on the PEDOT:PSS layer. More concentrated solutions of COP2 in ODCB determined the formation of a dark- red precipitate on the bottom of the vial. After baking films in a vacuum at 130°C for 15 min, the active layer film thicknesses measured by AFM were, respectively, 80, 100, 150, and 180 nm. Lastly, to create PSCs, 50 nm of Al was thermally deposited under a vacuum of 6×10^{-7} mmHg using an Edwards E306A vacuum coating apparatus. The active area of the cell was 0.25 cm^2. The current–voltage characteristics were measured using a Keithley 2401 source meter under the illumination of a Abet Technologies LS 150 Xenon Arc Lamp Source AM1.5 Solar Simulator, calibrated with an ILT 1400-BL photometer. The reported PCE results were the averaged values obtained from five different devices prepared under the same operative conditions. The spectral response of the solar cells was measured using a SCSpecIII (SevenStar Optics, Beijing, PRC) incident photon to charge carrier efficiency (IPCE) setup.

Synthesis of the Model Compound 1-Fullerenylhexane (HexF)

Scheme 1 outlines the experimental route for the preparation of HexF.

A solution of 0.837 g (5.07 mmol) of 1-bromohexane in 6 ml of anhydrous THF was added dropwise to 0.141 g (5.80 mmol) of Mg under stirring and in an inert atmosphere. The mixture was refluxed for 5 h, cooled down to room temperature, and then transferred via cannula to a solution of 1.22 g (1.69 mmol) of C_{60}-fullerene in 400 ml of anhydrous toluene and 2.30 ml of anhydrous *N,N*-dimethylformamide (DMF). The final mixture was reacted for 30 min under stirring at room temperature and in an inert atmosphere. The reaction was quenched with a solution of 100 mg of NH_4Cl in 10 ml of distilled water and then added to 200 ml of brine. The organic phase was washed with distilled water to neutrality, dried with $MgSO_4$, and concentrated. The crude product was dissolved in 50 ml of toluene and precipitated by adding 100 ml of MeOH dropwise to the solution. After filtration on a Teflon septum (0.45 μm pore size), 1.05 g of 1-fullerenylhexane (HexF) was recovered as a dark brown powder (77% yield).

^{1}H-NMR (400 MHz, $CDCl_3$, δ): 6.48 (s, 1H, $C_{60}H$), 3.45 (m, 2H, $C_{60}CH_2$), 2.60 (q, 2H, $C_{60}CH_2CH_2$), 1.92–1.45 (bm, 6H, central methylenes), 1.05 (t, 3H, CH_3).

^{13}C-NMR (100 MHz, $CDCl_3$, δ): 157.45 (2C, C_{60}), 153.91 (2C, C_{60}), 147.45 (1C, C_{60}), 147.42 (1C, C_{60}), 146.90 (2C, C_{60}), 146.31 (2C, C_{60}), 146.25 (2C, C_{60}), 146.15 (2C, C_{60}), 146.00 (2C, C_{60}), 145.78 (2C, C_{60}), 145.65 (2C, C_{60}), 145.41 (2C, C_{60}), 145.31 (2C, C_{60}), 145.25 (2C, C_{60}), 145.21 (2C, C_{60}), 144.77 (2C, C_{60}), 144.45 (2C, C_{60}), 143.22 (2C, C_{60}), 142.45 (2C+2C, C_{60}), 142.10 (2C, C_{60}), 141.95 (2C, C_{60}), 141.85 (2C, C_{60}), 141.78 (2C, C_{60}), 141.68 (2C, C_{60}), 141.55 (2C, C_{60}),141.45 (2C, C_{60}), 140.44 (2C, C_{60}), 140.00 (2C, C_{60}), 137.22 (2C, C_{60}), 135.85 (2C, C_{60}), 61.03 (1C, $C_{60}CH_2$), 41.82 (1C, $C_{60}CH_2$), 31.03 (1C, CH_2CH_3), 29.98 (1C, CH_2), 26.93 (1C, CH_2), 22.88 (1C, CH_2), 14.22 (1C, CH_2CH_3).

IR (KBr): $\nu = 2952$, 2921, 2850, 1428, 1384, 1182, 577, 526 cm^{-1}.

EIMS *m/z* (%): 807 (10) [M^+], 806 (25) [$M^+ - H$].

Synthesis of 3-(6-Fullerenylhexyl)thiophene (T6F)

Scheme 2 outlines the experimental route for the preparation of T6F.

1.24 g (5.07 mmol) of 3-(6-bromohexyl)thiophene prepared according to Ref. 14 in 6 ml of anhydrous THF was added dropwise to 0.141 mg (5.80 mmol) of Mg under stirring in an inert atmosphere. The mixture was refluxed for 5 h, cooled down to room temperature, and then transferred via cannula to a solution of 1.22 g (1.69 mmol) of C_{60}-fullerene in 400 ml of anhydrous toluene and 2.30 ml of anhydrous *N,N*-dimethylformamide (DMF). The final mixture was reacted for 30 min under stirring and in an inert atmosphere. The reaction was quenched with a solution of 100 mg of NH_4Cl in 10 ml of distilled water and then added to 300 ml of brine. The organic phase was washed with distilled water to neutrality, dried with $MgSO_4$, and concentrated. The crude product was dissolved in 75 ml of toluene and precipitated by adding 150 ml of *n*-pentane dropwise to the solution. After filtration on a Teflon septum (0.45 μm pore size), 1.20 g of 3-(6-fullerenylhexyl)thiophene (T6F) was recovered as a black powder with metallic lusters (80% yield).

^{1}H-NMR (400 MHz, ODCB-d_4, δ): 7.21 (m, 1H, H5Th), 6.93 (m, 2H, H2Th+H4Th), 6.48 (s, 1H, $C_{60}H$), 3.45 (m, 2H,

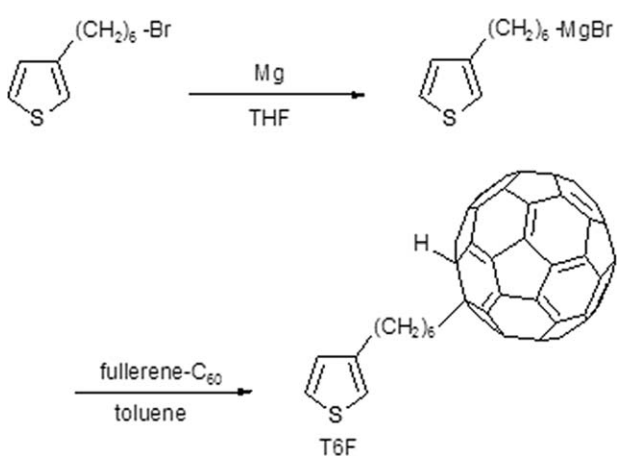

Scheme 2. Synthesis route for the preparation of T6F.

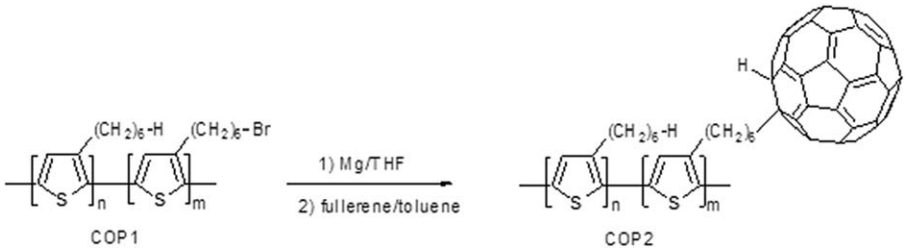

Scheme 3. Synthesis of copolymer COP2.

$C_{60}CH_2$), 2.85 (m, 2H, ThCH_2), 2.60 (m, 2H, $C_{60}CH_2CH_2$), 2.00–1.25 (bm, 6H, central methylenes).

^{13}C-NMR (100 MHz, ODCB-d_4, δ): 157.33 (2C, C_{60}), 153.22 (2C, C_{60}), 147.55 (1C, C_{60}), 147.33 (1C, C_{60}), 146.80 (2C, C_{60}), 146.42 (2C, C_{60}), 146.22 (2C, C_{60}), 146.11 (2C, C_{60}), 146.00 (2C, C_{60}), 145.75 (2C, C_{60}), 145.62 (2C, C_{60}), 145.45 (2C, C_{60}), 145.31 (2C, C_{60}), 145.22 (2C, C_{60}), 145.00 (2C, C_{60}), 144.67 (2C, C_{60}), 144.45 (2C, C_{60}), 143.18 (2C, C_{60}), 142.35 (2C+2C, C_{60}), 142.10 (2C, C_{60}), 141.95 (2C, C_{60}), 141.85 (2C, C_{60}), 141.78 (2C, C_{60}), 141.68 (2C, C_{60}), 141.53 (2C, C_{60}),141.43 (2C, C_{60}), 140.65 (2C, C_{60}), 140.11 (2C, C_{60}), 139.92 (1C, ThC3), 137.28 (2C, C_{60}), 135.98 (2C, C_{60}), 135.70 (1C, ThC5), 128.91 (1C, ThC2), 125.85 (1C, ThC4), 61.22 (1C, $C_{60}CH_2$), 41.62 (1C, $C_{60}CH_2$), 30.60 (1C, CH_2Th), 29.88 (1C, CH_2), 29.60 (1C, CH_2), 26.20 (2C, CH_2).

IR (KBr): $\nu = 3101$, 3051, 2924, 2851, 1512, 1461, 1427, 1173, 766, 671, 576, 526 cm^{-1}.

EIMS m/z (%): 889 (35) [M^+], 888 (60) [$M^+ - H$].

Synthesis of Poly[3-hexylthiophene-co-3-(6-bromohexyl)thiophene] (COP1)

1.02 ml of a CH_3MgCl 3.0*M* solution in anhydrous THF was added to 0.80 g (2.45 mmol) of 2,5-dibromo-3-hexylthiophene (2,5BT6H) and 0.25 g (0.61 mmol) of 2,5-dibromo-3-(6-bromohexyl)thiophene (2,5BT6Br) in 20 ml of anhydrous THF. The mixture was refluxed for 2 h under stirring in inert atmosphere and then 8.29 mg (0.015 mmol) of $NiDPPPCl_2$ was added and the reaction refluxed for 1 h. After cooling down to room temperature, the copolymer was recovered by adding 30 ml of methanol to the solution and subsequent filtration on a PTFE membrane (0.45 μm pore size). The copolymer was dissolved in 15 ml of $CHCl_3$ and reprecipitated with 50 ml of methanol, leading to 0.455 g (2.50 mmol, 82% yield) of dark-red COP1.

^{1}H-NMR (400 MHz, $CDCl_3$, δ): 6.98 (s, *H*4Th), 3.43 (t, CH_2Br), 2.90–2.45 (2bm, ThCH_2), 1.90–1.25 (bm, central methylenes), 0.89 (t, CH_3).

^{13}C-NMR (100 MHz, $CDCl_3$, δ): 140.29 (ThC3), 134.35 (ThC5), 131.30 (ThC2), 129.25 (ThC4), 34.63 (CH_2Br), 33.91 (CH_2CH_2Br), 30.91 (CH_2Th), 29.94 (CH_2), 29.30 (CH_2), 27.15 (CH_2), 22.91 (CH_2CH_3), 15.10 (CH_3).

IR (Ge): $\nu = 3050$, 2955, 2927, 2853, 1560, 1510, 1458, 1375, 1260, 1235, 1089, 830, 729, 643, 561 cm^{-1}.

Anal calcd for $[(C_{10}H_{13}BrS)_{0.2}\ (C_{10}H_{14}S)_{0.8}]_n$: C 65.97, H 7.64, Br 8.78, S 17.61; found: C 65.15, H 7.55, Br 8.95, S 18.35.

Synthesis of Poly[3-hexylthiophene-co-3-(6-fullerenylhexyl)thiophene] (COP2)

Scheme 3 shows the synthesis of the copolymer COP2.

0.407 g (2.24 mmol) of COP1 in 10 ml of anhydrous THF was added dropwise to 0.062 mg (2.56 mmol) of Mg under stirring in an inert atmosphere. The mixture was refluxed for 5 h, cooled down to room temperature, and then transferred via cannula to a solution of 0.539 g (0.747 mmol) of C_{60}-fullerene in 200 ml of anhydrous toluene and 1.10 ml of anhydrous *N*,*N*-dimethylformamide (DMF). The final mixture was reacted for 30 min under stirring in an inert atmosphere. The reaction was quenched with a solution of 50 mg of NH_4Cl in 5 ml of distilled water and then added to 150 ml of brine. The organic phase was washed with distilled water to neutrality, dried with $MgSO_4$, and concentrated. The copolymer was then fractionated by redissolving it in 75 ml of toluene and then slowly adding the solution to 150 ml of *n*-pentane. After filtration through a Teflon membrane (0.45 μm pore size), 0.571 g of fractionated COP2 was obtained (81% yield).

^{1}H-NMR (400 MHz, ODCB-d_4, δ): 7.00 (m, *H*4Th), 6.40 (s, $C_{60}H$), 3.45 (m, $C_{60}CH_2$), 2.80–2.55 (bm, ThCH_2 + $C_{60}CH_2CH_2$), 2.00–1.25 (bm, central methylenes), 0.95 (t, CH_3).

^{13}C-NMR (100 MHz, ODCB-d_4, δ): 157.43 (C_{60}), 153.50 (C_{60}), 147.92 (C_{60}), 147.15 (C_{60}), 146.95 (C_{60}), 146.52 (C_{60}), 146.31 (C_{60}), 146.15 (C_{60}), 146.05 (C_{60}), 145.85 (C_{60}), 145.65 (C_{60}), 145.50 (C_{60}), 145.35 (C_{60}), 145.25 (C_{60}), 145.05 (C_{60}), 144.75 (C_{60}), 144.35 (C_{60}), 143.10 (C_{60}), 142.45 (C_{60}), 142.20 (C_{60}), 141.90 (C_{60}), 141.80 (C_{60}), 141.70 (C_{60}), 141.62 (C_{60}), 141.55 (C_{60}),141.40 (C_{60}), 140.95 (ThC3), 140.68 (C_{60}), 140.15 (C_{60}), 137.25 (C_{60}), 135.95 (C_{60}), 135.15 (ThC5), 129.80 (ThC2), 126.80 (ThC4), 61.22 ($C_{60}CH_2CH_3$), 42.65 ($C_{60}CH_2$), 31.95 (CH_2CH_3), 30.55 (CH_2Th), 29.88 (CH_2), 29.63 (CH_2), 26.22 (CH_2), 14.55 (CH_2CH_3).

IR (Ge): $\nu = 3049$, 2954, 2923, 2851, 1538, 1460, 1428, 1377, 1173, 829, 576, 526 cm^{-1}.

Anal calcd for $[(C_{70}H_{14}S)_{0.2}\ (C_{10}H_{14}S)_{0.8}]_n$: C 85.12, H 4.55, S 10.33; found: C 84.85, H 4.65, S 10.50.

RESULTS AND DISCUSSION

The control of the morphology of the active layer in the polymeric photovoltaic cells is a very important parameter as it is necessary to maximize the surface area of the p–n junction to achieve a high energy conversion efficiency.[15,16] In fact, the

blend morphology can directly influence the conformational order of the conjugated backbone, while it is well known that a low degree of the polythiophene intra- and inter-chain disorder[17] may lead to a strong increase in hole mobility and, consequently, in charge carrier generation and extraction efficiency.[18]

Moreover, recently, some thin films of organic polymers have been deposited on ITO glass or plastic surfaces by ink-jet printing[19] or screen printing,[20] thus demonstrating that the development of fast, reproducible, homogeneous, and stable film-forming techniques is of the utmost interest.

In addition to a physical (thermal) approach, several chemical methods may also be used for controlling the morphology within the photoactive layer, to minimize the separation of the donor–acceptor compounds. One of these methods consists of synthesizing a conjugated p-type macromolecule bearing a fullerene molecule linked to its backbone. This method is particularly interesting and chemically elegant, as a single polymeric material would possess the ability to transport both the electrons and the holes (double-cable polymer). This would then lead to a fast inter- and intra-chain transport of positive holes and also to a more rapid displacement of the electrons along the fullerenes.[21] In addition, the interfacial area between the donor and acceptor would be maximized and segregation would be avoided. In this regard, J. R. Durrant *et al.* in a very recent paper,[22] stress the fact that the use of donor copolymers with a high degree of D–A character can be particularly effective in reducing the energy offset requirement for an efficient charge separation, thus leading to high efficient organic solar cell devices.

In this work, a new thiophenic monomer containing fullerene in the side chain was synthesized using the Grignard-coupling reaction; this synthesis method made it possible to use C_{60}-fullerene directly as the starting material, without either resorting to its expensive derivatives (e.g., PCBM) or preparing fulleropyrrolidine intermediates.[23] Moreover, the Grignard reaction involves few simple and straightforward steps, making the preparation of the monomer particularly easy, efficient, and interesting. Before proceeding to the synthesis of the fullerene-substituted thiophenic monomer, that is, 3-(6-fullerenylhexyl)thiophene (T6F), we attempted to synthesize a model compound, to verify the actual feasibility of synthesis. The monoaddition of the Grignard reagent to C_{60}-fullerene was inspired by the paper of Nakamura *et al.*[24] We started from 1-bromohexane, which is quite similar to 3-(6-bromohexyl)thiophene, but devoid of the thiophene moiety.

The reaction was performed in an inert atmosphere using freshly distilled anhydrous THF, by reacting 1-bromohexane with Mg turnings. The obtained mousey-gray Grignard solution was transferred via a PTFE cannula into a second flask containing the C_{60}-fullerene solubilized in toluene/DMF. The reaction mixture was left at room temperature for 15 min and then quenched with ammonium chloride; subsequently, the solvent was evaporated at reduced pressure. HexF was purified by fractionation using a toluene/methanol solution and recovered, after filtration, as a dark brown powder with a good yield.

The product obtained was characterized by ^{1}H- and ^{13}C-NMR, IR, and mass spectroscopy (see Experimental section).

The ^{1}H-NMR spectrum shows the expected signals; in details, the triplet ascribable to the terminal —CH_3 protons can be found at 1.05 ppm, the two quintets attributable to the internal —CH_2— protons of the alkyl chain between 1.45 and 1.92 ppm and the quintet due to the —CH_2— protons β to the fullerene group at 2.60 ppm. The multiplet at 3.45 ppm is relative to the —CH_2— directly linked to the fullerene: it is not a triplet due to the conformational stability of the alkyl chain linked to the fullerene; in fact, even if the bridge methylenic group is able to rotate, most of the time it maintains a specific conformation. This results in two hydrogen atoms that are chemically identical but magnetically different, whose couplings may be described by an AA′BB′ system, giving the observed characteristic peak profile.[25] Lastly, the singlet due to the directly fullerene-linked hydrogen can be found at 6.48 ppm. The ^{13}C-NMR spectrum, the IR spectroscopy and the mass analysis also confirm the HexF expected structure.

Once the ability to bind an alkyl halide directly to the fullerene via the Grignard reaction was confirmed, we proceeded with the synthesis of the monomer of interest (T6F). The reaction conditions used were analogous to those reported for the model compound, except for the purification conditions.

This time the ^{1}H-NMR spectrum was recorded in deuterated *o*-dichlorobenzene, as T6F is more soluble in this solvent than in chloroform (25 mg ml^{-1} vs. 8 mg ml^{-1}). Thanks to the previous study of the model compound, it was possible to state that the reaction was successful in this case also.

In particular, the singlet relative to the proton directly linked to fullerene is clearly visible at 6.48 ppm, the multiplet relative to the —CH_2— α and β to the fullerene group at 3.45 and 2.60 ppm, respectively, and the multiplet of the methylenic protons α to the thiophenic ring at 2.85 ppm. Lastly, the last three multiplets in the 1.25–2.00 ppm range are related to the central methylene groups of the alkylic side chain. Thiophenic aromatic protons appear partially embedded with the solvent signals and are found at 7.21 (H5) and 6.93 ppm (H2+H4).

The ^{13}C-NMR spectrum of the monomer is also in good agreement with the expected structure.

The presence of head-to-head (HH) couplings among the repeating units of poly(3-alkylthiophene)s affects the polymer conformation, leading to poor electrical conductivity,[26] low values of conjugation length,[27] and then low power conversion efficiencies in BHJ solar cells.[28] Therefore, we decided to polymerize T6F using a regiospecific procedure, namely the Grignard Metathesis (GRIM)[29] polymerization reaction, which involves the cross-coupling of organomagnesium intermediates prepared by reacting a 2,5-dibromothiophene derivative with a pre-formed Grignard's reactive (usually methylmagnesium chloride or isopropylmagnesium bromide) in the presence of a Ni(II) catalyst. Unfortunately, the dibromination of T6F to obtain 2,5-dibromo-3-(6-fullerenylhexyl)thiophene did not give any acceptable results as the bromination of the fullerene moiety was unavoidable even using mild reaction conditions, that

Table I. Copolymers Characteristics

Polymer	Yield[a] (%)	HT dyads[b] (%)	M_n[c] (kDa)	M_w/M_n
COP1	82	96	33.7	1.3
COP2	81	96	55.0	1.2

[a] In fractionated polymer.
[b] Regioregularity expressed as head-to-tail dyads percentage.
[c] Determined by GPC relatively to polystyrene standards.

is, adding the *N*-bromosuccinimide in two subsequent steps and operating at 0°C in anhydrous *N*,*N*-dimethylformamide.

An alternative procedure was then used, namely the insertion of the fullerenic substituent on a pre-synthesized polymeric precursor: a technique known as post-polymerization functionalization (PPF).[30]

As it may be inferred from the data reported in Table I, a satisfactory yield of the regioregular polymeric precursor COP1 was obtained by reacting 2,5-dibromo-3-hexylthiophene and 2,5-dibromo-3-(6-bromohexyl)thiophene in a 80 : 20 molar ratio with one equivalent of CH_3MgCl in anhydrous THF. The adopted synthetic strategy is not only easy to perform, but it also produces a polymer with appreciable molecular weight and microstructural features. COP1 is, in fact, characterized by a good DP_n (185 r.u.) and a high degree of regioregularity (96% in HT dyads content), as determined by the integral ratio of the signals at 2.90 and 2.45 ppm in the ^{1}H-NMR spectrum.[31]

COP1 was then dissolved in anhydrous THF and reacted with metallic Mg and then with a solution of fullerene in toluene using the same procedure used for the preparation of T6F from T6Br. After filtration, the resulting black powder was brought to dryness at 50°C in a vacuum oven. The high content of the non-functionalized monomer in COP2 allowed for both its good solubility in common organic solvents and its high post-polymerization functionalization reaction yield (86%).

The solubility of COP2 was 15 mg ml^{-1} in ODCB and 5 mg ml^{-1} in $CHCl_3$ and its molecular weight, determined via GPC with respect to polystyrene standards, was: $M_n = 55{,}000$ g mol^{-1} with a polydispersity index (PDI) of 1.2.

Figure 1 shows the ^{1}H-NMR spectrum of COP2.

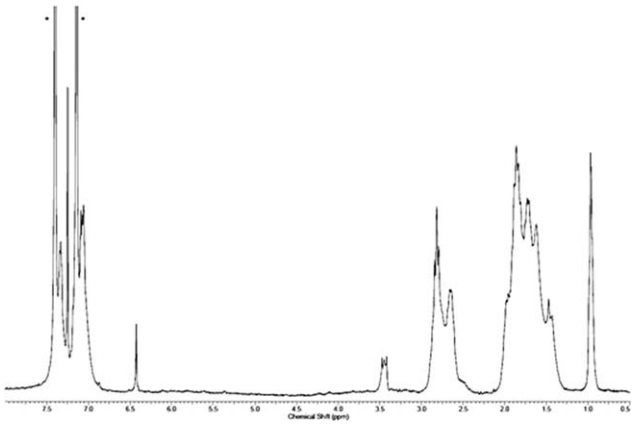

Figure 1. ^{1}H-NMR spectrum of COP2 in ODCB-d_4.

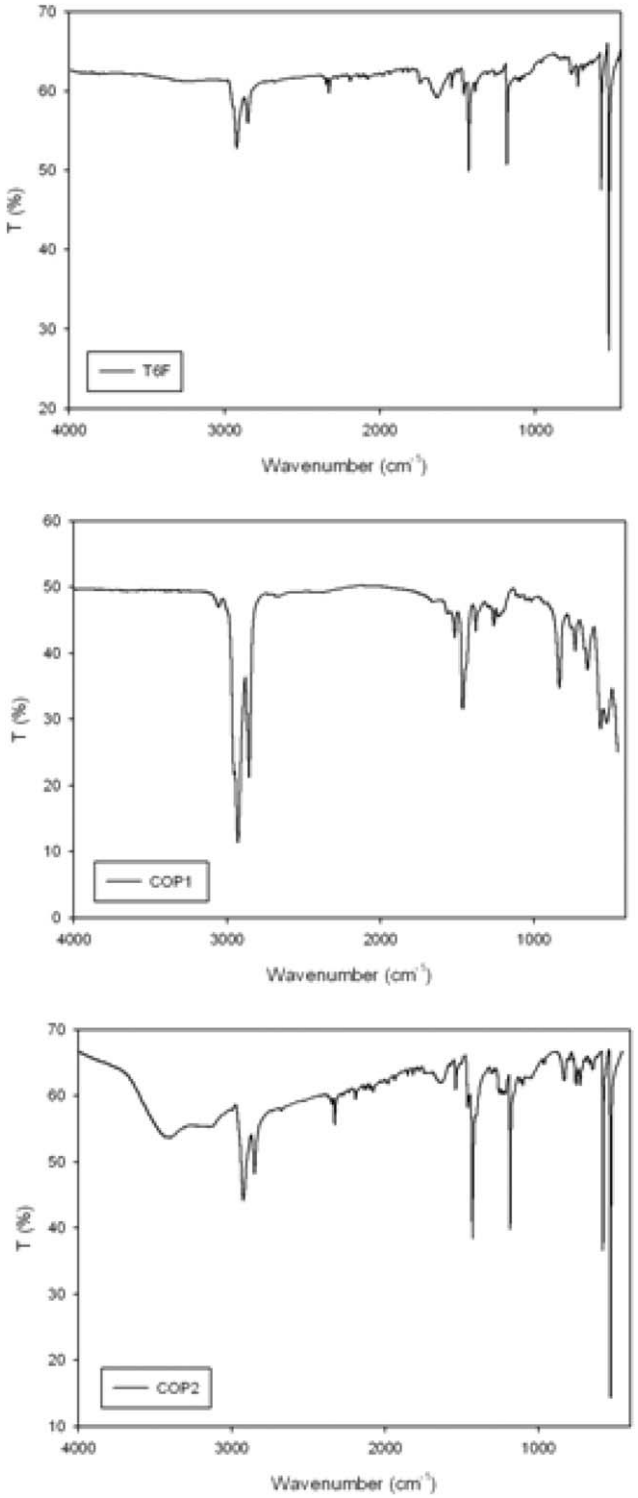

Figure 2. IR spectrum of T6F, COP1, and COP2.

The ^{1}H-NMR spectrum of COP2 shows the signals ascribable to both the monomers but some of them are superimposed as the two repeating units differ only in the final group of the side chain. However, some peaks can be unequivocally ascribed, like those at 0.95 ppm (protons of the terminal —CH_3 group of the alkyl chain of the non-functionalized monomer) and at 3.45

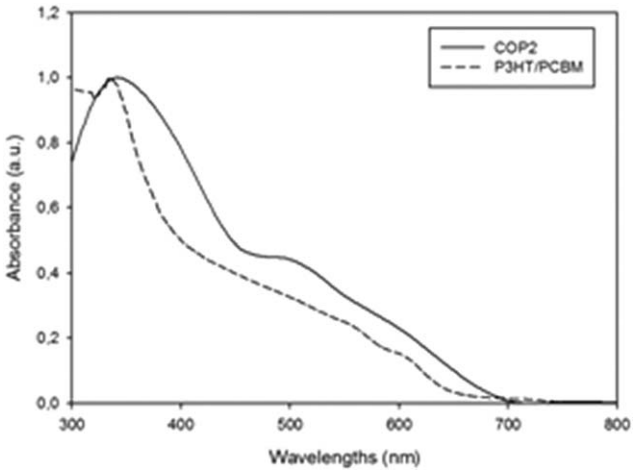

Figure 3. UV–Vis spectrum of COP2 and P3HT/PCBM in film.

ppm (—CH_2 directly linked to the fullerene). All signals between 1.25 and 2.00 ppm are due to the central methylenic groups of the alkyl chains of the two monomers. The multiplet in the range between 3.00 and 2.55 ppm is attributable to the signals of methylenic protons α- and β- to thiophene and fullerene, respectively. The overlapping of these signals makes it impossible to directly determine the regioregularity of the copolymer using ^{1}H-NMR.

At 6.40 ppm the signal of the proton directly attached to the fullerene group is evident and, lastly, in the aromatic region, the signal ascribable to thiophene H-4 can be found at 7.00 ppm.

The composition of COP2 was determined by comparing the integral of the signal of the —CH_3 group belonging to the alkylic monomer at 0.95 ppm with the integral of the peak at 3.45 ppm, concerning methylenes α to fullerene (this time, also, a multiplet and not a triplet), which is present only in the functionalized monomer. COP2 has a 20% molar content of T6F, thus proving the effectiveness of the used PPF reaction, as all —Br groups have been substituted by the C_{60} moiety.

As evidenced by ^{13}C-NMR analysis of COP2 (Supporting Information Figure S1), the signals at 34.63 and 33.91 ppm, ascribable to the presence of the —Br group in the side chains, clearly observable in COP1 spectrum, are completely missing in COP2 spectrum, thus confirming the complete bromine atom substitution by the fullerene group.

The signals reported in Experimental section confirm what was said about the proton spectrum. Moreover, the presence of only four evident signals ascribable to thiophenic carbons suggests the prevalence of one kind of configurational triad in the COP2 structure. This is not surprising, as the PPF reaction does not involve the polymer main chain but only the reactive functional groups at the end of the side chains.

Figure 2 shows the IR spectrum of T6F, COP1, and COP2 as a thin film on the Ge disk, while the main IR bands of the model compound, T6F, and copolymers COP1 and COP2 are listed in Supporting Information Table SI together with their respective assignments. The IR spectrum of the model compound HexF is also reported in Supporting Information Figure S2.

The IR analysis of the copolymers confirmed the expected structures. In fact, the characteristic absorptions of the 3-alkylthiophenic system are clearly evident, as well as those related to the particular functional groups, that is the halogen at 643 and 561 cm^{-1} and the fullerene moiety at about 1428, 1180, 576, and 526 cm^{-1}. Moreover, in the copolymers spectra, the band at 3101 cm^{-1} is absent, while that at about 3050 cm^{-1} is evident and the bands at 766 and 671 cm^{-1} are replaced by that at 829 cm^{-1}. These observations confirm that the repeating units of copolymers are linked through the α positions of thiophene rings (absence of α-β and β-β couplings), thus benefiting the structural regularity and electron delocalization.

Figure 3 shows the UV–Vis spectrum of COP2 and of P3HT/PCBM blend on a quartz slide cast from ODCB solution.

The absorbance around 340 nm is attributable to the fullerene derivative[32,33] (in the side chain, for COP2, and in the blend for P3HT) which, given the intense absorbance, appears to be a particularly efficient chromophoric system. The shoulder around 500 nm, particularly evident in COP2 spectrum, is attributable to the polythiophenic system while the presence of a further shoulder at 600 nm, albeit of weak intensity, indicates the formation of π-stacking between thiophene rings.[34] Even if COP2 is a copolymer between two thiophenes bearing different groups in the side chain—one of which is particularly bulky—the structured profile of the spectrum clearly evidences the presence of a conformational order among the polymeric main chains.

The DSC thermogram of COP2 (Supporting Information Figure S3) shows an evident endothermic flexure at 29°C (glass transition temperature) and two endothermic peaks at 95°C and 155°C which are ascribable to the melting of crystalline domains determined by the packing of side chains and backbones, respectively. It is interesting to note that, for the usually used poly(3-hexylthiophene) (rrP3HT, Aldrich Chemical, %HT dyads >95%, M_n: 15,000–45,000, CAS No. 156074-98-5, Code No. 698989), the main chain melting transition occurs at around 200°C and the T_g at −4.7°C,[35,36] while COP2 has a

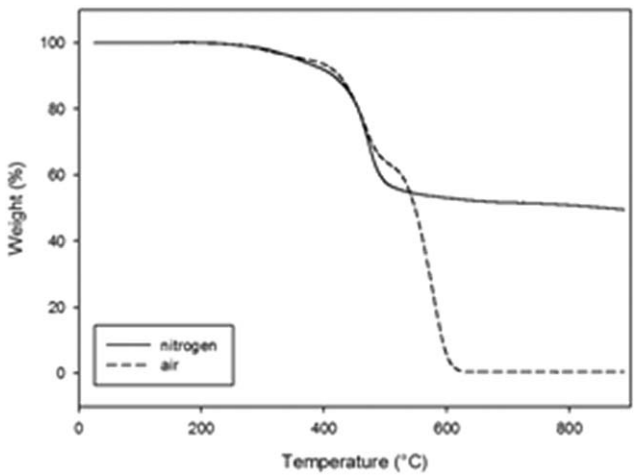

Figure 4. TGA graphs of COP2 under nitrogen and in air.

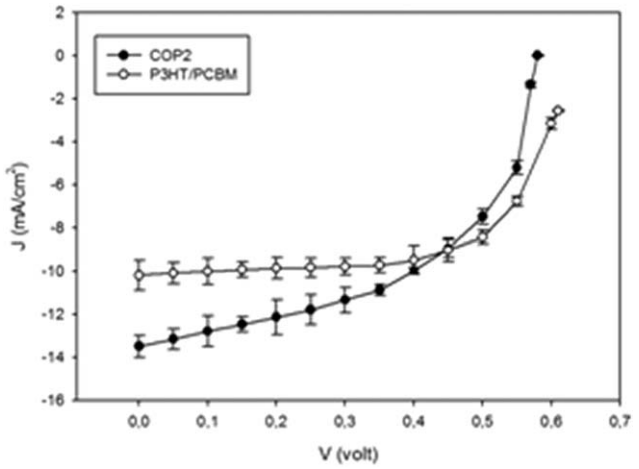

Figure 5. Current density–voltage for tested cells under AM 1.5 one-sun illumination. For the copolymer the curve relating to the most performing cell is reported.

lower T_m but a higher T_g than the reference polymer; the selection of polymers with the highest possible glass transition temperature is an important prerequisite for the thermal stability of the photoactive blend to avoid the demixing of its components.[37,38] The lower T_m of COP2 with respect to the reference polymer can be ascribed to the higher steric hindrance of the substituent of the former, as bulky groups in polythiophene side chains generally hinder the crystallization process of the polymer.[39] Moreover, the higher T_g of COP2 can be explained in terms of the reduced mobility of the side chains, as already evidenced in the ^{1}H-NMR section (vide infra).

The COP2 thermal stability was investigated by the TGA analysis both under nitrogen and in air at a heating scan of 20°C min^{-1}. The thermograms obtained are shown in Figure 4.

In nitrogen, COP2 is stable up to around 300°C, after which the thermal decomposition begins with a two-step weight loss. The second step begins at around 400°C. In air, the decompositions start at around 275°C and the second step always at 400°C. This time, a third degradation step can be observed and, over 600°C, no residual product can be found. These results agree with those obtained by Kumar *et al.*,[40] showing that the addition of carbon nanotubes or C_{60} fullerene to poly(3-hexylthiophene) reduces its thermal stability.

Figure 5 shows the *J–V* characteristic curves of solar cells which have the structure of ITO/PEDOT:PSS/photoactive layer/Al under AM 1.5 one sun illumination (100 mW cm^{-2}).

As reference cell we used a P3HT/PCBM 1 : 1 weight ratio, as some studies have shown that devices with this ratio achieve the highest power conversion efficiency.[41,42] The cell made with COP2 did not require the use of PCBM, as fullerene was already present in this copolymer, at a loading of approximately 46 wt %. We tried to optimize the deposition conditions of the active layers by acting both on the thickness of the blend and on the annealing temperature. In fact, these important parameters directly affect the PCE of the final device through the light absorption efficiency as well as the morphology of the photoactive blend, mainly acting on the J_{SC} of the PSC.[43] The effect of the thickness of the active layer was examined by depositing, using the doctor blade, COP2 solutions in ODCB at different concentrations (Table II). The thermal annealing of the photoactive layer was performed at 130°C for 15 min in a vacuum, as these conditions gave the best results. The best conditions for the reference cell were found to be: P3HT:PCBM 1 : 1 (w/w) and 15 wt % solution in ODCB, leading to a 160-nm-thick film after doctor blade deposition.

A summary of the averaged *J–V* characteristics, based on the analysis of five devices, is given in Table II.

The results obtained for the P3HT/PCBM device are in good agreement with those reported in the literature; in fact, we obtained a 3.53% of PCE with a 160-nm-thick film, after an annealing time of 15 min at 130°C, whereas the best conditions reported for the same system were an annealing time of 10 min at 130°C using a 150-nm-thick film, giving a 3.60% of PCE.[43] In the COP2 case, the best results were obtained with a 150 nm thick film with the same annealing conditions used for the reference cell, leading to a superior PCE performance of 4.19%.

The IPCE plots of the best devices under short circuit conditions are shown in Figure 6.

The photo–current response wavelength of the cells based on the P3HT/PCBM photoactive blend and on the COP2 layer range from 290 to 700 nm and 310 to 750 nm, respectively. The curve of the device based on the reference cell has two feature peaks at 355 and 575 nm and a shoulder at 600 nm, whereas the device based on the copolymer shows only two peaks at 400 and 580 nm. The IPCE profile of COP2 follows the trend observed in the absorption spectra of the copolymer in film, indicating that the harvested photons over the whole absorption spectrum contribute to the photocurrent. Moreover, an enhanced quantum efficiency is observed in the device made with COP2 as compared to the device made with P3HT/PCBM,

Table II. Photovoltaic Parameters for the Devices Obtained Using the Two Different Photoactive Polymers

Polymer	Concentration (mg ml^{-1})	Thickness (nm)	J_{sc} (mA cm^{-2})	V_{oc} (V)	FF (%)	PCE (%)
COP2	7	80	6.50	0.58	50.2	1.89 ± 0.08
COP2	10	100	10.7	0.58	52.0	3.23 ± 0.12
COP2	13	150	13.5	0.58	53.2	4.19 ± 0.18
COP2	15	180	11.6	0.58	51.3	3.45 ± 0.11
P3HT/PCBM	15	160	10.20	0.63	55.0	3.53 ± 0.12

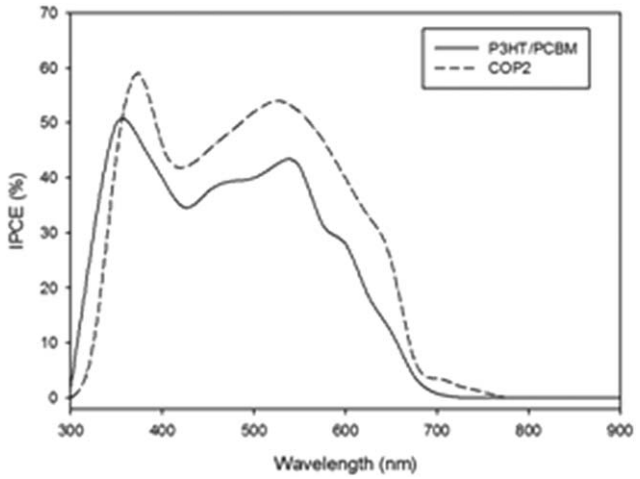

Figure 6. IPCE curves of the prepared OPV solar cells.

thus suggesting an improved charge collection efficiency of the copolymer.

The results obtained clearly show that the performance of the double-cable based solar cells is higher than that of the device prepared following the conventional bulk-heterojunction approach, and reaches a PCE higher than the value reported in literature for BHJ solar cells made with poly(alkyl)thiophenes (P3ATs)/PCBM with a conventional architecture (3.57%).[44]

To analyze the morphology of solar cells, we chose to use atomic force microscopy (AFM). Figure 7 shows the surface morphology of the reference blend, that is P3HT and PCBM (1 : 1 weight ratio) as well as of a film of COP2 on ITO glass. The two films had similar thickness (about 150 nm) and were prepared by filming with doctor blade the ODCB solutions of polymers on ITO glasses that had been cleaned beforehand using the same procedure used for the preparation of solar cells. After the film deposition, samples were subjected to an annealing procedure (15 min at 130°C under vacuum) and surface images were recorded using an AFM in a non-contact (tapping) mode in height-modulated (HMM) mode.

The AFM images of the surfaces of the two prepared films are quite different; in fact the surface rms (root-mean-square) roughness is 16.1 nm for the P3HT:PCBM film (with an average 25.6 nm diameter of grains) and 5.7 nm for COP2 (average 7.1 nm diameter grains). The bumps in topography are ascribable to PCBM-rich domains. P3HT has a rougher surface than COP2, thus suggesting a higher degree of self-organization in the blend, which could foster the formation of ordered structure in the film.[45] However, fullerene derivatives that have a strong tendency to self-crystallize (such as PCBM) do not mix well with P3HT, thus producing inhomogeneous composite films with a less efficient photoinduced charge-transfer[46] and then a lower J_{SC}.[47] Therefore, the use of COP2 as a photoactive blend, with no need for other EA species, is very promising, as the copolymer produces films with a very smooth surface, a more uniform molecular distribution, and a high interfacial area of the electron donor–acceptor domains, which acts positively on the final J_{SC} and PCE, as confirmed by the data shown in Table II. Further studies are in progress, with the aim to prepare regioregular copolymers with a fullerene content higher than COP2.

CONCLUSIONS

In this work, we have obtained important results toward the optimization and production of polymeric solar cells. The first goal we had set provided for the synthesis of a model compound that confirmed the feasibility of the direct functionalization of a bromoalkane with the fullerene moiety. After the confirmation that the model could be obtained, the synthesis was modified by replacing 1-bromohexane with 3-(6-bromohexyl)thiophene, thus obtaining the monomer 3-(6-fullerenylhexyl) thiophene with a good yield and via a simple and straightforward synthesis procedure. The designed synthesis was adopted to prepare a soluble and filmable copolymer functionalized with 20% (in moles) of fullerene which provided a 4.19% photovoltaic efficiency when used as the photoactive layer in a polymeric solar cell, after a suitable optimization of the layer thickness and of the annealing procedure. The PCE obtained is higher than that of the reference cell and also of the values reported in literature for conventional BHJ solar cells based on the P3AT/PCBM system. The results obtained are especially encouraging. In fact, they show the possibility to obtain a photoactive polymer that is directly usable, without resorting to the preparation of the EA/ED blend (polymer/fullerene, carbon nanotubes or PCBM), thus avoiding the problems associated with the

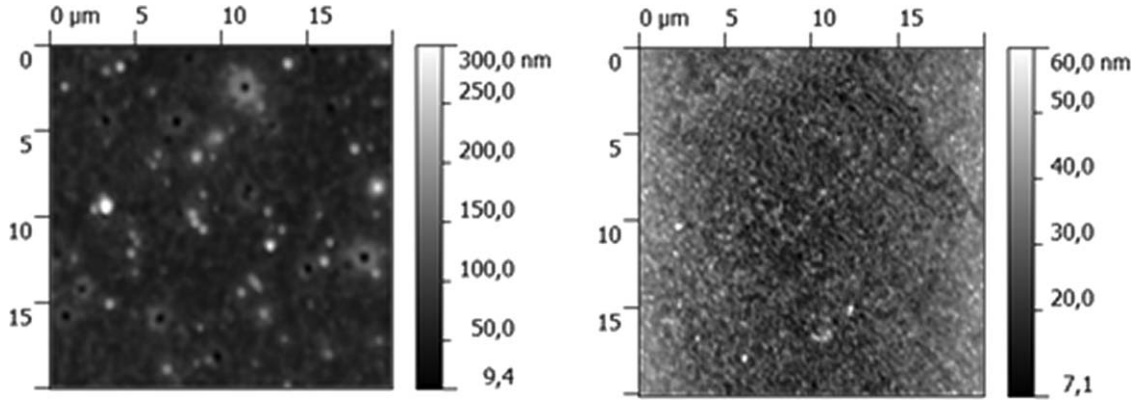

Figure 7. AFM images of a P3HT/PCBM blend (left) and of a COP2 film (right).

aggregation, segregation, and inhomogeneity of the components in the photoactive layer.

ACKNOWLEDGMENTS

Italian PRIN 2010–2011 is gratefully acknowledged.

REFERENCES

1. White, M. S.; Olson, D. C.; Shaheen, S. E.; Kopidakis, N.; Ginley, D. S. *Appl. Phys. Lett.* **2006**, *89*, 143517.
2. Waldauf, C.; Morana, M.; Denk, P.; Schilinsky, P.; Coakley, K.; Choulis, S. A.; Brabec, C. J. *Appl. Phys. Lett.* **2006**, *89*, 233517.
3. Niggermann, M.; Glatthaar, M.; Lewer, P.; Mueller, C.; Wagner, J.; Gombert, A. *Thin Solid Films* **2006**, *511–512*, 628.
4. Carlé, J. E.; Krebs, F. C. *Sol. Energy Mater. Sol. Cells* **2013**, *119*, 309.
5. Liu, Y.; Larsen-Olsen, T. T.; Zhao, X.; Andreasen, B.; Sondergaard, R. R.; Hegelsen, M.; Norrman, K.; Jorgensen, M.; Krebs, F. C.; Zhan, X. *Sol. Energy Mater. Sol. Cells* **2013**, *112*, 157.
6. Vandewal, K.; Himmelberger, S.; Salleo, A. *Macromolecules* **2013**, *46*, 6379.
7. Tan, Z.; Hou, J.; He, Y.; Zhou, E.; Yang, C.; Li, Y. *Macromolecules* **2007**, *40*, 1868.
8. Li, M.; Xu, P.; Yang, J.; Yang, S. *J. Mater. Chem.* **2010**, *20*, 3953.
9. Cravino, A.; Sedar Sariciftci, N. *J. Mater. Chem.* **2002**, *12*, 1931.
10. Lanzi, M.; Paganin, L.; Errani, F. *Polymer* **2012**, *53*, 2134.
11. Moon, J. S.; Takacs, C. J.; Cho, S.; Coffin, R. C.; Kim, H.; Bazan, G. C.; Heeger, A. *J. Nano Lett.* **2010**, *10*, 4005.
12. Glowacki, E. D.; Sariciftci, N. S.; Tang, C. W. In Solar Energy; Richter, C. et al., Eds.; Springer: New York, **2013**.
13. Jeffries, M.; Sauvé, G.; McCullough, R. D. *Adv. Mater.* **2004**, *16*, 1017.
14. Lanzi, M.; Paganin, L. *React. Funct. Polym.* **2010**, *70*, 346.
15. Moulé, A. J.; Meerholz, K. *Adv. Funct. Mater.* **2009**, *19*, 3028.
16. Jorgensen, M.; Norman, K.; Krebs, F. C. *Sol. Energy Mater. Sol. Cells* **2008**, *92*, 686.
17. Zerbi, G.; Radaelli, R.; Veronelli, M.; Brenna, E.; Sannicolò, F.; Zotti, G. *J. Chem. Phys.* **1993**, *98*, 4531.
18. Turner, T. S.; Pingel, P.; Steyrleuthner, R.; Crossland, E. J. W.; Ludwigs, S.; Neher, D. *Adv. Funct. Mater.* **2011**, *21*, 4640.
19. Jørgensen, M.; Norman, K.; Gevorgyan, S. A.; Tromholt, T.; Andreasen, B.; Krebs, F. C. *Adv. Mater.* **2012**, *24*, 580.
20. Krebs, F. C.; Jørgensen, M.; Norman, K.; Hagemann, O.; Alstrup, J.; Nielsen, T. D.; Fyenbo, J.; Larsen, K.; Kristensen, J. *Sol. Energy Mater. Sol. Cells* **2009**, *93*, 422.
21. Falkenberg, C.; Uhrich, C.; Olhof, S.; Maennig, B.; Riede, M.; Leo, K. *J. Appl. Phys.* **2008**, *104*, 34506.
22. Dimitrov, S. D.; Durrant, J. R. *Chem. Mater.* **2014**, *26*, 616.
23. Prato, M.; Maggini, M. *Acc. Chem. Res.* **1998**, *31*, 519.
24. Matsuo, Y.; Iwashita, A.; Abe, Y.; Li, C. Z.; Matsuo, K.; Hashiguchi, M.; Nakamura, E. *J. Am. Chem. Soc.* **2008**, *130*, 15429.
25. Bax, A. In Two-Dimensional Nuclear Magnetic Resonance in Liquids; Reidel, D., Ed.; Springer Verlag: Berlin, Germany, **1982**.
26. Ho, H.; Leclerc, M. *J. Am. Chem. Soc.* **2003**, *125*, 4412.
27. Brédas, J. L. *J. Chem. Phys.* **1985**, *82*, 3809.
28. Kudret, S.; Kesters, J.; Janssen, S.; Van den Brande, N.; Defour, M.; Van Mele, B.; Manca, J.; Lutsen, L.; Vanderzande, D.; Maes, W. *React. Funct. Polym.* **2014**, *75*, 22.
29. McCullough, R. D.; Lowe, R. D. *J. Chem. Soc. Chem. Commun.* **1992**, 70.
30. Lanzi, M.; Paganin, L.; Costa Bizzarri, P.; Della Casa, C.; Fraleoni, A. *Macromol. Rapid Commun.* **2002**, *23*, 630.
31. Sato, M.; Morii, H. *Macromolecules* **1991**, *24*, 1196.
32. Bondouris, B. W.; Molins, F.; Blank, D. A.; Frisble, C. D.; Hillmyer, M. A. *Macromolecules* **2009**, *42*, 4118.
33. Cugola, R.; Giovanella, U.; Di Gianvincenzo, P.; Bertini, F.; Catellani, M.; Luzzati, S. *Thin Solid Films* **2006**, *511*, 489.
34. Lanzi, M.; Paganin, L. *Eur. Polym. J.* **2008**, *44*, 3987.
35. Motaung, D. E.; Malgas, G. F.; Arendse, C. J.; Mavundla, S. E.; Oliphant, C. J.; Knoesen, D. *Sol. Energy Mater. Sol. Cells* **2009**, *93*, 1674.
36. Bertho, S.; Haeldermans, L.; Swinnen, A.; Moons, W.; Martens, T.; Lutsen, L.; Vanderzande, D.; Manca, J.; Senes, A.; Bonfiglio, A. *Sol. Energy Mater. Sol. Cells* **2007**, *91*, 385.
37. Ma, W.; Yang, C.; Gong, X.; Lee, K.; Heeger, A. J. *Adv. Funct. Mater.* **2005**, *15*, 1617.
38. Lindqvist, C.; Wang, E.; Andersson, M. R.; Mueller, C. *Macromol. Chem. Phys.* **2014**, *215*, 530.
39. Schopf, G.; Kossmehl, G. In Polythiophenes-Electrically Conductive Polymers; Springer Verlag: Berlin, Germany, **1997**.
40. Kumar, J.; Singh, R. K.; Kumar, V.; Rastogi, R. C.; Singh, R. *Diamond Relat. Mater.* **2007**, *16*, 446.
41. Chirvase, D.; Parisi, J.; Hummelen, J. C.; Dyakonov, V. *Nanotechnology* **2004**, *15*, 1317.
42. Li, G.; Shrotriya, V.; Yao, Y.; Yang, Y. *J. Appl. Phys.* **2005**, *98*, 043704.
43. Ho, C.; Huang, E.; Hsu, W.; Lee, C.; Lai, Y.; Yao, E.; Wang, C. *Synth. Met.* **2012**, *162*, 1164.
44. Chi, D.; Qu, S.; Wang, Z.; Wang, J. *J. Mater. Chem. C* **2014**, *2*, 4383.
45. Li, G.; Shrotriya, V.; Huang, J. S.; Yao, Y.; Moriatry, T.; Emery, K.; Yang, Y. *Nat. Mater.* **2005**, *4*, 864.
46. Hiramoto, M.; Fujiwara, H.; Tokoyama, M. *Appl. Phys. Lett.* **1991**, *58*, 1062.
47. Savagatrup, S.; Printz, A. D.; Rodriquez, D.; Lipomi, D. J. *Macromolecules* **2014**, *47*, 1981.